Design, Analysis, and Validation of Synergetic Control for Active Stabilisation Systems

Saranya Mukherjee[1] and Mansi[1] and Anjan Kundu[2]

[1] Graduate Student, Institute of Radio Physics and Electronics, University of Calcutta
[2] Associate Professor, Institute of Radio Physics and Electronics, University of Calcutta

Abstract. This work presents the design and analysis of a hexapod-based active stabilisation system for subsea sensor payloads, using a Stewart platform configuration. A novel scissor actuator mechanism is introduced to achieve cost-effectiveness, precision, and ease of maintenance. Kinematic modelling, supported by static and dynamic analyses, is performed to evaluate torque requirements, range of motion, and velocity characteristics. A synergetic nonlinear control law is developed to ensure smooth dynamics, rapid convergence under 0.2s, and robustness against external disturbances, without overshoot, oscillation, or chattering, while achieving a negligible steady-state error of under 0.001%. The control law proposed implicit actuator synchronisation for significantly reduced computational effort(upto 6 times per cycle) in real-time applications. Simulation studies validate the effectiveness of the integrated design, demonstrating reliable stabilisation across multiple degrees of freedom, with promising implications for deployment in autonomous and remotely operated vehicles.

1 Introduction

Stewart platform, also known as a hexapod, is a parallel manipulator consisting of six actuators arranged between a fixed base and a movable platform[5, 8]. Its architecture enables motion in six degrees of freedom, three translational and three rotational, making it highly suitable for applications requiring precise positioning and stabilisation.

Stabilisation refers to the process of maintaining a desired orientation or position in the presence of external disturbances. In subsea environments, stabilisation is critical for sensor payloads, as ocean currents, waves, and mechanical vibrations, all combined with the inherent fact that the seabed is uneven and can cause positioning error, can compromise measurement accuracy. Passive stabilisation methods, such as rigid supports or damping structures, offer limited effectiveness under dynamic conditions. On the contrary, active stabilisation employs actuators and control systems to continuously counteract disturbances, ensuring precise alignment and positioning.

In most cases, classic PID or Linear Quadratic Regulator(LQR) systems are used in order to achieve stabilisation on either each actuator's position or the platform's position as a whole[12]. Since the Stewart platform's forward kinematics are very computationally expensive, typically the control laws are applied on the individual actuators for real-time implementation. Although the LQR systems improve on the Active Disturbance Rejection Control(ADRC)[10] by over 30-40%, they suffer from having to be finely tuned to work well.

Scheme	**Reference**	**Convergence Time**(s)	**Tracking Error**	**Benefit**
Sliding-Mode Control (SMC)	[16, 11]	NA	$< 0.8\%$	Finite Constraint Handling
Classical / Linear Controllers (PID, LQR, State Feedback)	[10]	1.5s	$< 1\%$	Disturbance rejection
Fuzzy Logic Controllers (FLC)	[3]	3s	NA	Online parameter adaptation
Neural-Network Based Control	[2]	1.2s	$< 2.5\%$	Learning-based
PROPOSED	NA	0.2s	$< 0.001\%$	Implicit actuator synchronization

Table 1: Comparison of major control schemes

Fuzzy logic controllers[15] have been used both as standalone control schemes and as online parameter tuning models for classic models like LQR to make them more adaptive. The online tuning model suffers from higher computational costs and raises the convergence time of the model it is paired with.

Learning models[7, 16], on the other hand, have the benefit and adaptability of being a neural learning model, but again suffer from high computation costs.

Sliding mode control[6, 13] comes the closest to synergetic control, but falls short due to its prominent chattering problems and instability even when exposed to low amounts of noise.

All of these models need a secondary supervisory and synchronisation layer in order to ensure that the motion does not conflict with the safety barriers; this comes with a very high computation cost. But our proposed synergetic control model provides implicit actuator synchronisation with minimal computation, often reducing it by 6 times per cycle. This emerges as a major differentiating point when it comes to real-time implementations, which will necessitate the enforcement of safety barriers.

In this work, we have integrated the Stewart platform with a novel scissor actuator mechanism. The scissor design, driven by servo motors, provides extreme cost-effectiveness yet precise actuation. Combined with nonlinear synergetic control, the system enables real-time compensation across all six degrees of freedom, ensuring robust stabilisation for sub-sea sensor payloads.

Section 2 proposes a novel actuator design and its kinematic and torque characteristics. Section 3 proposes the synergetic control law for the actuator. Section 4 analyses the results of the control law in the perspective of both the individual actuators and the platform's motion as a whole.

2 Actuator Design

2.1 Basic framework

The fundamental framework of the proposed actuator design is shown in Fig. 1. The mechanism adopts a scissor configuration with four arms of length L, joined at a central pivot by two longer arms of length 2L. The servo (blue rectangle in the centre) varies the angle β. This variation in angle adjusts the length H of the actuator.

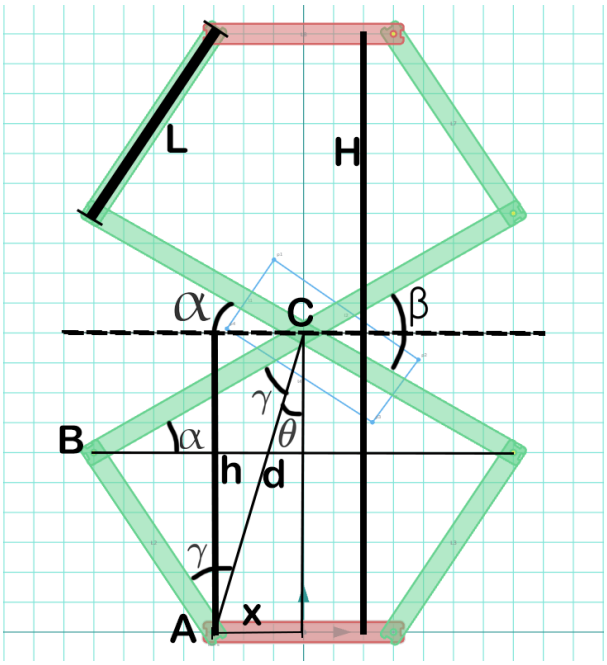

Fig. 1: Geometry of the scissor mechanism showing each term.

2.2 IK equations

Fig. 1 shows the geometry of the scissor mechanism. From the figure, we shall focus on the triangle ABC; using the cosine rule, we get:

$$\cos\gamma = \frac{L^2 + d^2 - L^2}{2Ld} = \frac{d}{2L} \tag{1}$$

Given that $\cos\gamma = \cos(\frac{\pi}{2} - \alpha - \theta) = \sin(\alpha + \theta)$, we have:

$$\alpha + \tan^{-1}\left(\frac{x}{h}\right) = \sin^{-1}\left(\frac{d}{2L}\right) \tag{2}$$

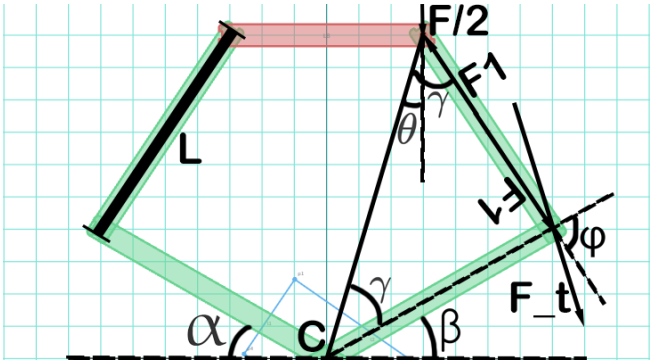

Fig. 2: Free body diagram of the proposed mechanism.

From this, we can solve for α:

$$\alpha = \sin^{-1}\left(\frac{\sqrt{x^2+h^2}}{2L}\right) - \tan^{-1}\left(\frac{x}{h}\right) \tag{3}$$

Finally, we can compute β as:

$$\beta = 2\left[\sin^{-1}\left(\frac{\sqrt{x^2+\frac{H^2}{4}}}{2L}\right) - \tan^{-1}\left(\frac{2x}{H}\right)\right] \tag{4}$$

Equation 4 gives us the inverse kinematics equation for the scissor mechanism, which shall serve as the basis for the control of each actuator in the Stewart platform.

2.3 FK equations

From Fig. 1, we can use the sine rule in triangle ABC to get:

$$h = L\sin\alpha + L\sqrt{1 - \frac{(L\cos\alpha - x)^2}{L^2}} \tag{5}$$

Hence, we can compute H as:

$$H = 2L\left[\sin\frac{\beta}{2} + \sqrt{1 - \frac{(L\cos\frac{\beta}{2} - x)^2}{L^2}}\right] \tag{6}$$

Fig. 3 shows system parameters for the actuator.

2.4 Static analysis

We need to compute the torque required at the servo motor to hold the platform at a certain height H. Fig. 2 shows the free body diagram of the scissor mechanism.

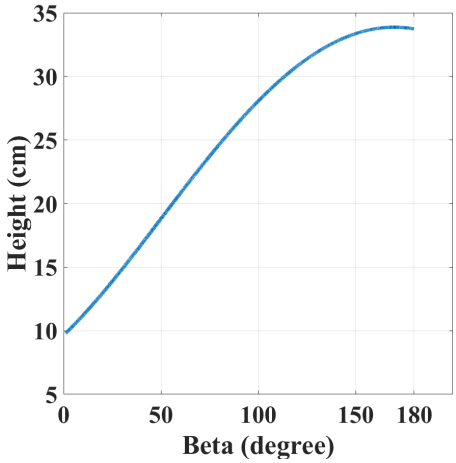

(a) Actuator length H vs β

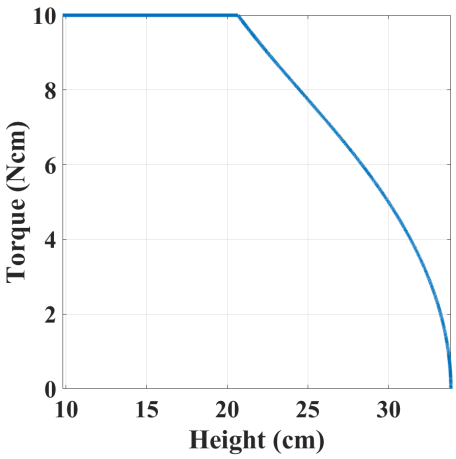

(b) Torque on Servo τ vs H

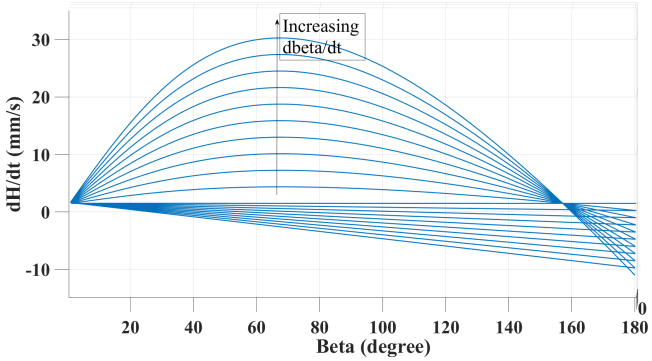

(c) dH/dt vs β for varying $d\beta/dt$

Fig. 3: System parameters for actuator with $L = 8.5cm, x = 1.5cm$

Assuming that a force F acts at the centre of the platform, since the mechanism is symmetrical about the vertical axis, each half will experience a force of $F/2$.

Balancing forces at the top platform link,

$$F_1 \cos(\gamma - \theta) = \frac{F}{2} \tag{7}$$

Forces acting on the middle link will be F_1 on both sides for the link to be at equilibrium.

$$F_t = \frac{F \sin\gamma \cos\gamma}{cos(\gamma - \theta)} \tag{8}$$

Now, given that the link has a length L and the torque is distributed evenly on both sides,

$$\tau = \frac{F \cdot L \sin\left(2 * (\theta + \alpha)\right)}{\sin\left(2\theta + \alpha\right)} = \frac{2L \cdot F \sin(2\gamma)}{\sin\alpha} \tag{9}$$

Where, $\theta = \tan^{-1}\left(\frac{2x}{H}\right),\ \gamma = \cos^{-1}\left(\frac{d}{2L}\right),\ and\ d = \sqrt{x^2 + \frac{H^2}{4}}$.

2.5 Dynamic analysis

Differentiating Equation 6 with respect to time gives us the velocity relationship:

$$\frac{dH}{dt} = \frac{d\beta}{dt}\left[L \cdot \cos\frac{\beta}{2} + \frac{1}{\sqrt{1 - \frac{(L\cos\frac{\beta}{2} - x)^2}{L^2}}} \cdot \sin\frac{\beta}{2}\left(L\cos\frac{\beta}{2} - x\right)\right] \tag{10}$$

Similarly, differentiating Equation 4 with respect to time gives us:

$$\frac{d\beta}{dt} = \left(\frac{H}{4L} \cdot \frac{1}{\sqrt{1 - \frac{x^2 + \frac{H^2}{4}}{4L^2}} \cdot \sqrt{x^2 + \frac{H^2}{4}}} + \frac{4x}{4x^2 + H^2}\right)\frac{dH}{dt} \tag{11}$$

3 Control system for actuator

Synergetic Control Theory (SCT) is adopted to design the nonlinear control system for the proposed actuator. SCT shapes system behaviour[1] by forcing its states toward an invariant manifold, ensuring smooth closed-loop dynamics without chattering.

We define the macro-variable that computes the error in the actuator:

$$\sigma = H_f - H \tag{12}$$

where H_f is the desired actuator length and H is the current length. This macro-variable represents the position error. The invariant manifold is defined as:

$$T \cdot \dot{\sigma} + \theta = 0 \tag{13}$$

where $\theta = f(\sigma)$ is a nonlinear function of σ, and T is a fixed design parameter controlling convergence speed. This represents a first-order decay function, denoting the smooth manifold along which the system will converge. θ can be chosen with the following constraints:

- invertible and differentiable
- $\theta(0) = 0$
- $\sigma \cdot \theta(\sigma) > 0$ for all $\sigma \neq 0$

We have chosen:

$$\theta = \sigma \tag{14}$$

From eqn. 13,

$$T \cdot \left[\frac{dH_f}{dt} - \frac{dH}{dt}\right] + [H_f - H] = 0 \tag{15}$$

Since H_f is constant for position control,

$$T \cdot \left[-\frac{dH}{dt} \right] + [H_f - H] = 0 \tag{16}$$

Now, substituting eqn. 6 and 10,

$$T \cdot \left[-\frac{d\beta}{dt} \left[L \cdot \cos\frac{\beta}{2} + \frac{1}{\sqrt{1 - \frac{(L\cos\frac{\beta}{2} - x)^2}{L^2}}} \cdot \sin\frac{\beta}{2} \left(L\cos\frac{\beta}{2} - x \right) \right] \right] + \left[H_f - 2L \left[\sin\frac{\beta}{2} + \sqrt{1 - \frac{(L\cos\frac{\beta}{2} - x)^2}{L^2}} \right] \right] = 0 \tag{17}$$

Now, solving for $\frac{d\beta}{dt}$,

$$\frac{d\beta}{dt} = \frac{1}{T \cdot \left[L \cdot \cos\frac{\beta}{2} + \frac{1}{\sqrt{1 - \frac{(L\cos\frac{\beta}{2} - x)^2}{L^2}}} \cdot \sin\frac{\beta}{2} \left(L\cos\frac{\beta}{2} - x \right) \right]} \cdot \left[H_f - 2L \left[\sin\frac{\beta}{2} + \sqrt{1 - \frac{(L\cos\frac{\beta}{2} - x)^2}{L^2}} \right] \right] \tag{18}$$

Finally, we use eqn. 18 to get the control law after enforcing the dynamic limitations of a commodity servo motor.

$$\max|\dot{\beta}(t)| = 250^\circ/s = 4.36 rad/s$$
$$\max|\ddot{\beta}(t)| = 4583.66^\circ/s^2 = 80 rad/s^2$$
$$\beta[k+1] = \beta[k] + \frac{d\beta}{dt} \cdot \Delta t \tag{19}$$

Where $\beta[k]$ is the servo angle at time step k, Δt is the sampling time, and $\beta[k+1]$ is the updated servo angle to be sent to the servo motor. Fig. 4a shows the time domain response for a single actuator when the SCT law and the servo constraints are enforced.

4 Results

4.1 Case study 1

Vertical motion of the platform from $z = 25$ cm to $z = 29.4$ cm is considered. Only one direction of twist is considered here for simplicity. We analyse the platform motion with respect to each of the actuators moving simultaneously. Fig. 4 shows the simulation results of the platform motion for one direction of twist. It demonstrates the effectiveness of the SCT-based actuator dynamics in reflecting the same smooth manifold onto the overall platform motion accurately. The following design parameters can be calculated:

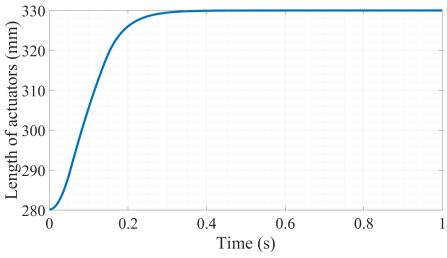

(a) Actuator length $\mathbf{L}$ vs Time

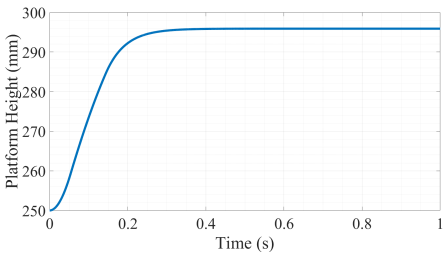

(b) Platform vertical position Z vs Time

Fig. 4: Platform motion vs time for one direction of twist

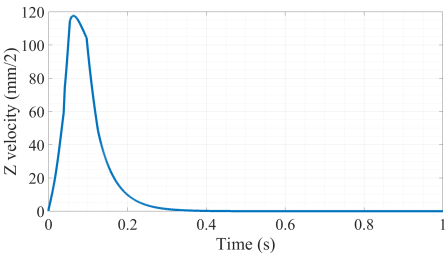

(a) Z velocity of the platform $\mathbf{J}(3)$ vs Time

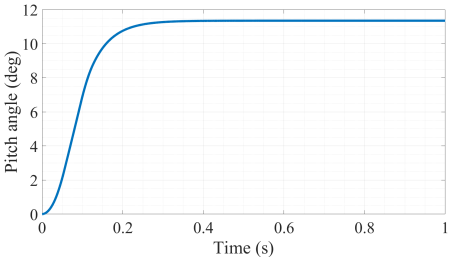

(b) Platform pitch vs Time

Fig. 5: Platform motion vs time for three directions of twists

- Convergence time(2%): 0.2s
- Tracking error: 0.00089% after 2s

4.2 Case study 2

The twisting motion of the platform along all axes is considered simultaneously. The platform is twisted from an initial orientation of $[0°,\ 0°,\ 0°]$ to $[-3.5°,\ 11.3°,\ 31.4°]$, along with a vertical displacement from $z = 25$ cm to $z = 26.1$ cm, with minimal twist in the translational X and Y directions. Here, we analyse all the twist directions of the platform and their corresponding dynamics. Fig. 5 shows the simulation results of the platform motion for three directions of twist.

4.3 Analysis

We can derive the motion of the platform with respect to the motion of the actuators by computing its Jacobian[4]. Using eqn. 10, we can compute $\frac{dH}{dt}$ as a function of $\frac{d\beta}{dt}$.

$$\dot{\mathbf{L}} = \frac{1}{T}\left[H_f - H\right] = \frac{1}{T}\left[H_f - 2L\left[\sin\frac{\beta}{2} + \sqrt{1 - \frac{(L\cos\frac{\beta}{2} - x)^2}{L^2}}\right]\right] \tag{20}$$

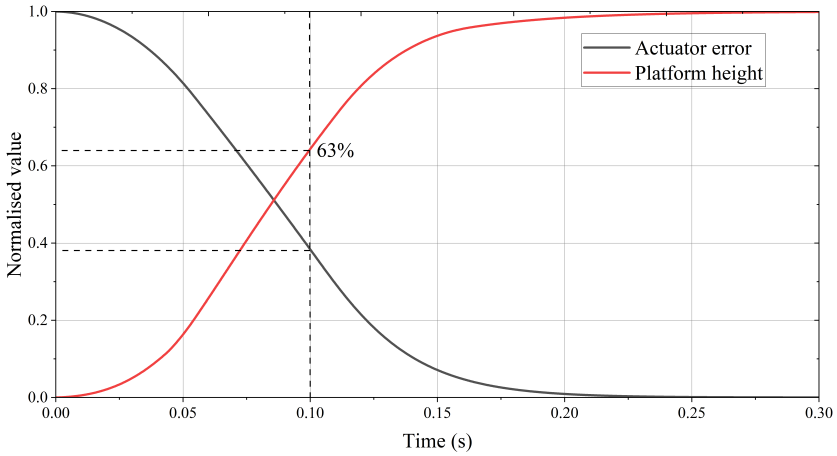

Fig. 6: Normalised actuator and platform motion

$$\mathbf{v} = \mathbf{J}^T(\mathbf{J}\mathbf{J}^T + \lambda^2\mathbf{I})^{-1} \cdot \frac{1}{T}\left[H_f - 2L\left[\sin\frac{\beta_i}{2} + \sqrt{1 - \frac{(L\cos\frac{\beta_i}{2} - x)^2}{L^2}}\right]\right]_{i=1}^{6} \tag{21}$$

where $\mathbf{v}$ is the velocity matrix of the platform, $\mathbf{J}$ is the Jacobian of the system, and λ is the damping factor introduced to stabilise the inversion[9, 14]. The velocity is then integrated to compute the position of the platform in real-time. The Jacobian ($\mathbf{J}$) is a 6x6 matrix,

$$\mathbf{J} = \begin{bmatrix} \hat{\mathbf{L}}_1^T & \hat{\mathbf{L}}_1^T[\mathbf{R}\cdot\mathbf{P}_1] \\ \hat{\mathbf{L}}_2^T & \hat{\mathbf{L}}_2^T[\mathbf{R}\cdot\mathbf{P}_2] \\ \vdots & \vdots \\ \hat{\mathbf{L}}_6^T & \hat{\mathbf{L}}_6^T[\mathbf{R}\cdot\mathbf{P}_6] \end{bmatrix} \tag{22}$$

where $\mathbf{L}$ is the leg velocity and $\mathbf{R}$ is the rotation vector of the current pose,

$$\mathbf{P}_i^{world} = \mathbf{R}\cdot\mathbf{P}_i^{local} + \mathbf{T} \tag{23}$$

As evident from eqn. 21, the velocity of the platform is directly related to the control law. Since the control law is just a first-order decay function, we can generalise this to a form like,

$$y(t) = y_0\, exp\left[-\frac{t}{T}\right] \tag{24}$$

Where y_0 is the initial value and T is the time constant from eqn. 13, and $y(t)$ is subject to the same limiting conditions as $\dot{\beta}(t)$ and $\ddot{\beta}(t)$. So, we can reduce eqn. 21 to such a decay equation for each degree of freedom for real-time tracking. Fig. 6 shows the normalised motion of the actuator and the platform as a whole; it shows that both the individual actuators and the platform's motion follow the same nature of the curve while having the exact same time constant. This serves as a major leg up over other control

schemes in terms of computational effort. Comparing Tables 2,3, we can see that the control law not only has an exceptional time response, but also speeds up computation by $\sim 5.5 - 6$ times per computation cycle.

Operation	**FLOPs**
Build J	$\sim$50
Compute $J^T J$ 6x6	216
Add $\lambda^2 I$	6
Matrix inversion (Cholesky)	$\sim$250-300
Compute $J^T \dot{L}$	36
Matrix multiply	36
Total	$\sim$600-650

Table 2: FLOPs for traditional method

Operation	**FLOPs**
Decay calculation	$\sim$10
First derivative	2
Clamp check	2
Second derivative	2
Clamp check	2
Total	18 * 6 = 108

Table 3: FLOPs for proposed method

5 Conclusion

This work demonstrates a novel control strategy for a Stewart platform. The Synergetic control law achieves smooth and robust actuator behaviour, achieving fast convergence to the desired position without overshoot, oscillation, or chattering, while achieving negligible steady-state error. We have also proposed a novel, extremely low-cost scissor-mechanism linear actuator as an alternative to conventional linear actuators for such applications. Comprehensive inverse and forward kinematics models, followed by static and dynamic analysis, demonstrated that the synergetic control law can be effectively applied to both the actuators and the platform as a whole. The combination of these offers an implicit synchronisation of actuators, which lends itself to very low computational costs compared to other schemes. Overall, the proposed actuator design, together with the SCT-based control frame- work, provides a strong foundation for realising a compact and actively stabilised Stewart platform.

6 Future scope

Future developments may focus on experimental validation in complex environments, integrated with real-time sensor feedback, and optimisation of actuator geometry for enhanced efficiency and analysing the performance of the control algorithm in noisy enviornments. Extending the control framework to adaptive and fault-tolerant schemes will further improve robustness. Additionally, scaling the design for deployment in autonomous underwater vehicles and advanced marine survey systems offers significant potential for practical applications.

References

[1] Ahifar, A., Ranjbar Noee, A., Rahmani, Z.: Terminal synergetic design of a nonlinear robot manipulator in the presence of disturbances. COMPEL-The international journal for computation and mathematics in electrical and electronic engineering **37**(1), 208–223 (2018)

[2] Barhaghtalab, M.H., Sepestanaki, M.A., Mobayen, S., Jalilvand, A., Fekih, A., Meigoli, V.: Design of an adaptive fuzzy-neural inference system-based control approach for robotic manipulators. Applied Soft Computing **149**, 110970 (2023). https://doi.org/https://doi.org/10.1016/j.asoc.2023.110970, https://www.sciencedirect.com/science/article/pii/S1568494623009882

[3] Bouhamatou, Z., Abedssemed, F.: Fuzzy synergetic control for dynamic car-like mobile robot. Acta Mechanica et Automatica **16**(1), 48–57 (2022). https://doi.org/10.2478/ama-2022-0007, https://doi.org/10.2478/ama-2022-0007

[4] Buss, S.R.: Introduction to inverse kinematics with jacobian transpose, pseudoinverse and damped least squares methods. IEEE Journal of Robotics and Automation **17**(1-19), 16 (2004)

[5] Dasgupta, B., Mruthyunjaya, T.: The stewart platform manipulator: a review. Mechanism and machine theory **35**(1), 15–40 (2000)

[6] Keshtkar, S., Poznyak, A.S., Hernandez, E., Oropeza, A.: Adaptive sliding-mode controller based on the "super-twist" state observer for control of the stewart platform. Automation and Remote Control **78**(7), 1218–1233 (2017)

[7] Ko, B., Park, J.W., Kim, D.W.: A study on iterative learning control for vibration of stewart platform. International Journal of Control, Automation and Systems **15**(1), 258–266 (2017)

[8] LUPULESCU, P.S.A.E.: Studies on stewart platform–a review

[9] Nakamura, Y.: Advanced robotics: redundancy and optimization. Addison-Wesley Longman Publishing Co., Inc. (1990)

[10] Qu, X., Li, Z., Chen, Q., Peng, C., Wang, Q.: Research on improved active disturbance rejection control strategy for hydraulic-driven stewart stabilization platform. Industrial Robot: the international journal of robotics research and application **51**(6), 881–889 (2024)

[11] Safeena, M., Jiji, K., et al.: Control of stewart platform using adaptive smooth integral sliding mode algorithm. ISA transactions **156**, 99–108 (2025)

[12] Silva, D., Garrido, J., Riveiro, E.: Stewart platform motion control automation with industrial resources to perform cycloidal and oceanic wave trajectories. Machines **10**(8), 711 (2022)

[13] Velasco, J., Calvo, I., Barambones, O., Venegas, P., Napole, C.: Experimental validation of a sliding mode control for a stewart platform used in aerospace inspection applications. Mathematics **8**(11), 2051 (2020)

[14] Willoughby, R.A.: Solutions of ill-posed problems (an tikhonov and vy arsenin). Siam Review **21**(2), 266 (1979)

[15] Zahedi, F., Zahedi, Z.: A review of neuro-fuzzy systems based on intelligent control. Journal of Electrical and Electronic Engineering **3**(2-1), 58–61 (2015). https://doi.org/10.11648/j.jeee.s.2015030201.23, https://doi.org/10.11648/j.jeee.s.2015030201.23

[16] Zhao, J., Xu, Z., Wu, D., Cao, Y., Xie, J.: Six-dof stewart platform motion simulator control using switchable model predictive control. arXiv preprint arXiv:2503.11300 (2025)